

Current Biology, Volume 33

Supplemental Information

Systematic analysis of RhoGEF/GAP localizations uncovers regulators of mechanosensing and junction formation during epithelial cell division

Florencia di Pietro, Mariana Osswald, José M. De las Heras, Inês Cristo, Jesús López-Gay, Zhimin Wang, Stéphane Pelletier, Isabelle Gaugué, Adrien Leroy, Charlotte Martin, Eurico Morais-de-Sá, and Yohanns Bellaïche

Figure S1: Libraries and tagged RhoGEF/GAP localizations in interphase, related to Figure 1.

Unless otherwise indicated, in all images, ‘xy’ indicates apical confocal top views at the level of the AJ in the notum and FE, while ‘yz’ denotes apical-basal confocal sections for the notum, and midsagittal view of the egg chamber. MyoII:3xmKate2 is shown in magenta. All images in E-K correspond to cells in interphase.

(A) Overview of the transgenic lines generated to characterize the fluorescently tagged RhoGEF/GAP localizations.

(B) Schematics describing the use of the donor and guide plasmid library to generate RhoGEF/GAP loss of function alleles that can be modified to produce tagged or sequence specific alleles.

(C) Dorsal view of *Drosophila* pupa at 14 hours after pupa formation (hAPF) (top, left from⁸⁴). The black box in the top panel indicates the whole notum tissue. xy image of MyoII:3xmKate2 and Ecad:GFP in the notum (bottom, left). xy (middle) and yz (right) images of the MyoII:3xmKate2 (top and bottom) and Ecad:GFP (top) distributions in interphase cells in the notum. Dashed line: position of the yz section.

(D) Images of MyoII:3xmKate2 (left, middle and right) and Ecad:GFP (left and middle) in midsagittal (yz, top) and surface (xy, bottom) views of a stage 4 egg chamber. The middle and right panels correspond to close-ups in the regions outlined in the left panels.

(E) xy images of Cysts:GFP, RhoGEF2:GFP, RhoGAP71E:GFP, Spg:GFP, Conu:GFP (top and bottom) and MyoII:3xmKate2 (top) in the notum.

(F) yz (top) and xy (bottom) images of Cysts:GFP, RhoGEF2:GFP and Conu:GFP in the FE.

(G) xy (left) and yz (right) images of RhoGAP19D:GFP (top and bottom) and MyoII:3xmKate2 (top) in the notum.

(H) yz (top) and xy (bottom) images of RhoGAP19D:GFP in the FE.

(I) yz (top) and xy (bottom) images of RtGEF:GFP in the FE.

(J) xy images at the level of the nucleus of Pbl:GFP and Tum:GFP in the notum.

(K) xy images of Tum: GFP (left and right) and Cell membrane marker (left) in the FE. Images correspond to projection of the nuclei and ring canals.

Scale bars: 5µm

See also Figure S2, Methods S1A-D and Data S1A,B and [website](#).

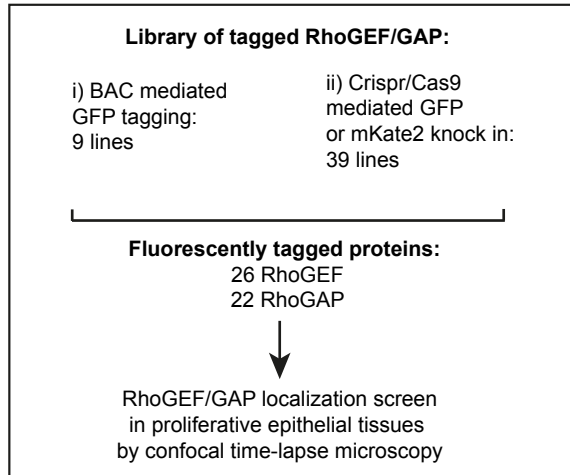
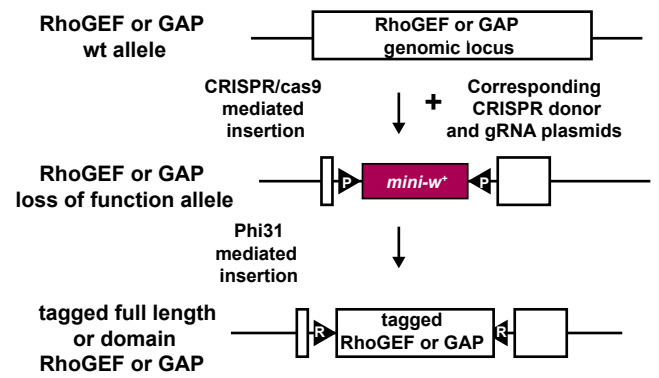
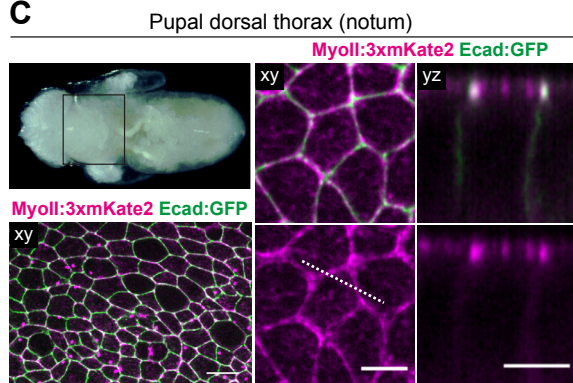
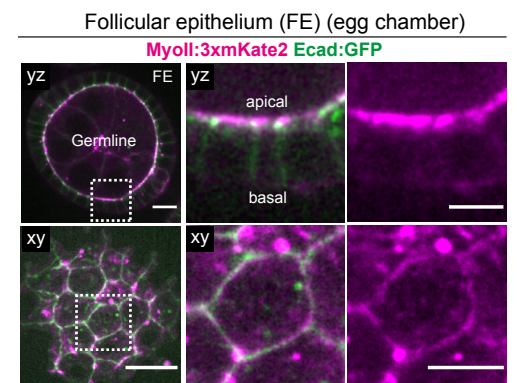
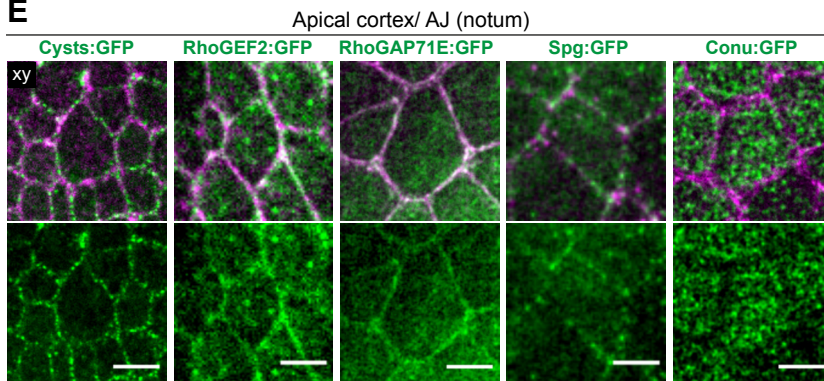
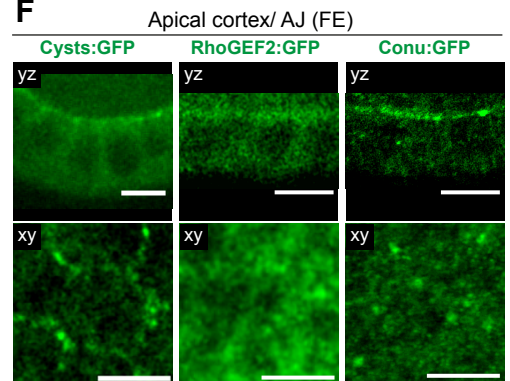
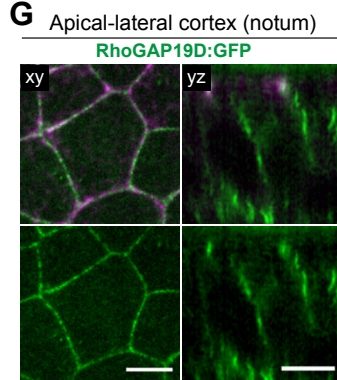
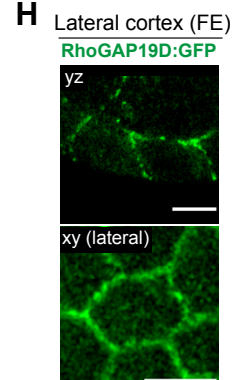
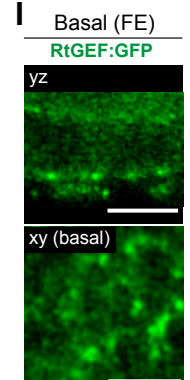
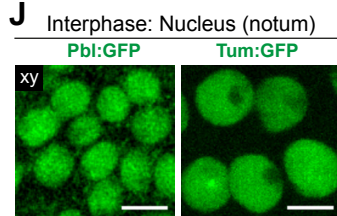
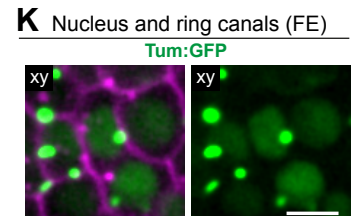
A**B****C****D****E****F****G****H****I****J****K**

Figure S2: Localizations of tagged RhoGEF/GAPs in interphase, related to Figure 1.

Unless otherwise indicated, for all images, 'xy' indicates apical confocal top views at the level of the AJ in the notum and FE, while 'yz' denotes apical-basal confocal sections for the notum, and midsagittal views of the FE. MyoII:3xmKate2 is shown in magenta. All images correspond to cells in interphase.

(A, B) Schematics of a notum (A) and a FE (B) epithelial cell with the subcellular localizations of RhoGEF/GAPs in interphase. RhoGEF/GAPs are color-coded according to their localization. Only the RhoGEF/GAPs observed with a sufficient signal to noise ratio in the notum or the FE are shown.

(C) xy images of Graf:GFP, CdGAPr:GFP, RhoGAP1A:GFP, Exn:GFP (top and bottom) and MyoII:3xmKate2 (top) in the notum.

(D) yz (top) and xy (bottom) images of Graf:GFP, Ziz:GFP, Zir:GFP, CG46491:GFP and Mbc:GFP in the FE.

(E) xy images of GEFMeso:GFP, Sos:GFP (top and bottom) and MyoII:3xmKate2 (top) in the notum epithelium. Yellow arrowheads: Sos:GFP accumulations at the apical TCJ.

(F) yz (left) and xy (right, confocal section taken 4μm below the AJ) images of Cdep:GFP (top and bottom) and MyoII:3xmKate2 (top) in the notum. White arrowhead: Cdep enrichment at basolateral TCJ.

(G) yz (top) and xy (bottom) images of CdGAPr:GFP, RhoGAP1A:GFP and RhoGAP15B:GFP in the FE.

(H) yz (left, top) and xy (left, bottom) images of Cdep:GFP; xy images of RhoGAP5A:GFP (right, top and bottom), and MyoII:3xmKate2 (right, top) in the basal cortex of the FE.

(I) xy images of Mbc:GFP, RhoGAP5A:GFP (top and bottom) and MyoII:3xmKate2 (top) in the notum. White arrowheads: Mbc:GFP and RhoGAP5A:GFP accumulations at the apical TCJ.

(J) xy time-lapse images of RhoGAP5A:GFP (top and bottom) and MyoII:3xmKate2 (top) during the junction elongation phase of a cell-cell rearrangement in the notum. White arrowheads: RhoGAP5A:GFP accumulation. Time is in min.

(K) xy images at the level of the nucleus of RhoGAP54D:GFP, CdGAPr:GFP, CG43102:GFP and RhoGEF4:GFP in the notum.

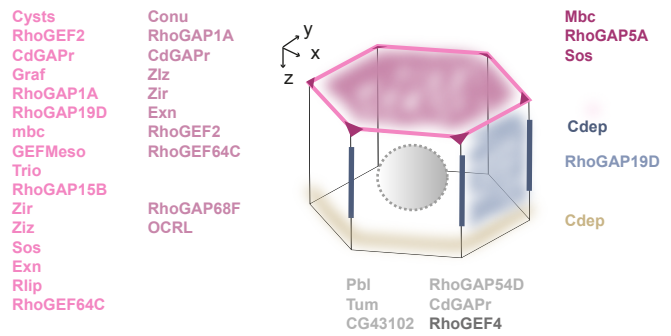
(L) xy images at the level of the nucleus of RhoGAP54D:GFP, RhoGEF4:GFP (top and bottom) and Nup107:RFP (top) in the FE.

Scale bars: 5μm

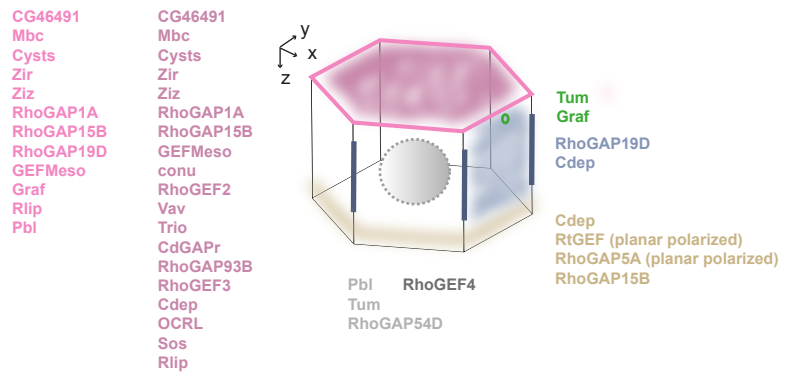
See also Figure S1, Methods S1A,B, Data S1A,B, Video S1 and the [website](#).

A

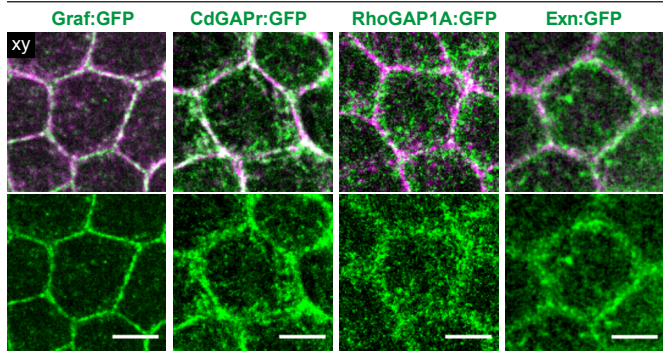
Interphase- notum

**B**

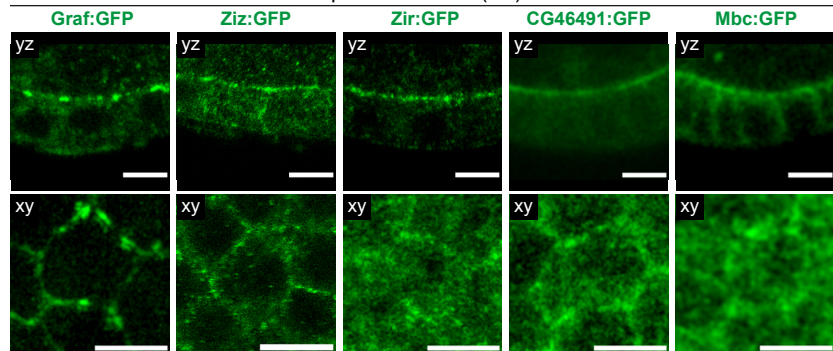
Interphase- FE (stages 2-6)

**C**

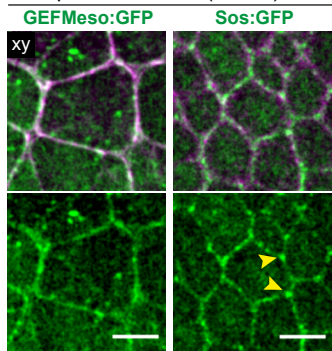
Apical cortex/ AJ (notum)

**D**

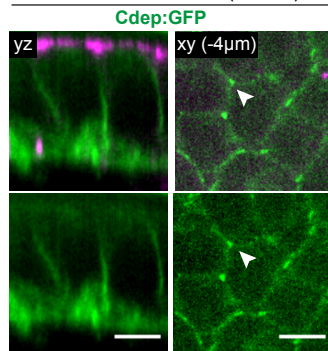
Apical cortex/ AJ (FE)

**E**

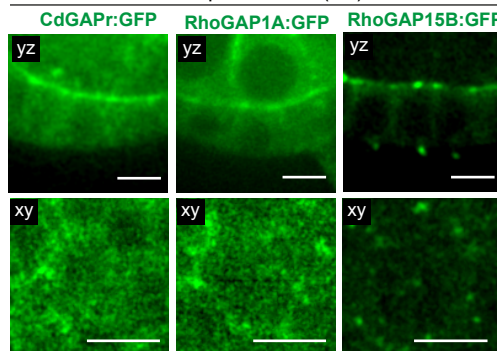
Apical cortex/ AJ (notum)

**F**

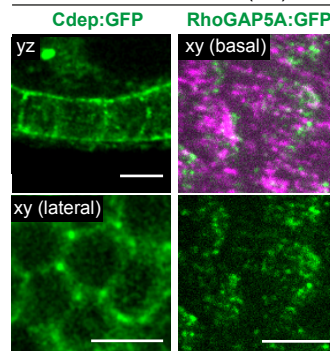
Basolateral cortex (notum)

**G**

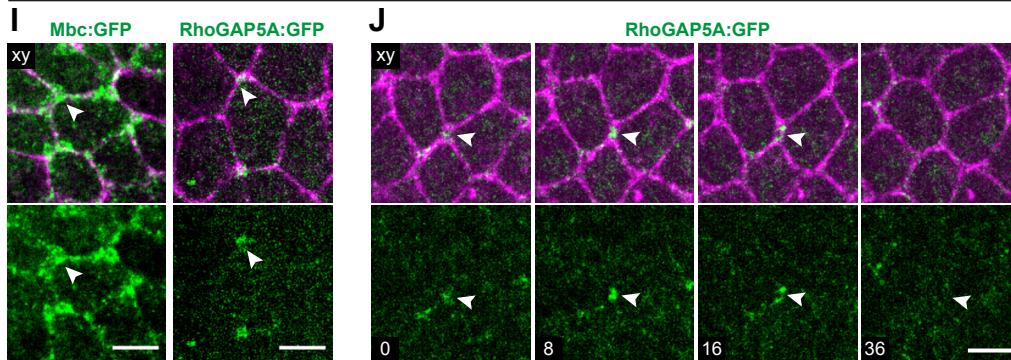
Apical cortex (FE)

**H**

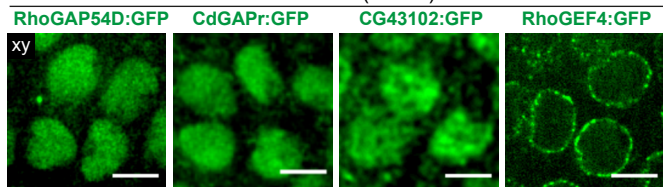
Basolateral cortex (FE)



Apical vertex, rearranging vertex (notum)

**K**

Nucleus (notum)

**L**

Nucleus (FE)

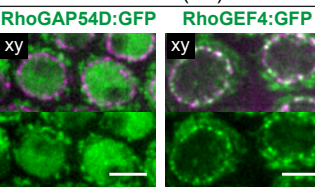


Figure S3: Localizations of additional RhoGEF/GAPs during epithelial cell division, related to Figure 1.

Unless otherwise indicated, ‘xy’ indicates apical confocal top views at the level of the AJ in the notum and FE, while ‘yz’ denotes apical-basal confocal section at the level of the cytokinetic ring or the midbody for the notum, and midsagittal view of the egg chamber. MyoII:3xmKate2 is shown in magenta.

(A) xy time-lapse images of Pbl:GFP (top and bottom) and MyoII:3xmKate2 (top) during cell division in the notum. Time (min, indicated in the lower left image corner) is set to 0 at the onset of cytokinesis marked by the initial deformation of AJ by the constriction of the cytokinetic ring.

(B) xy time-lapse images of Tum:GFP (top and bottom) and MyoII:3xmKate2 (top) during cell division in the notum. White arrowheads: Position of the contractile ring and midbody respectively. Time (min, indicated in the lower left image corner) is set to 0 at the onset of cytokinesis marked by the initial deformation of AJ by the constriction of the cytokinetic ring.

(C) xy images at level of the nucleus of RhoGAP68F:GFP, RhoGAP1A:GFP, Rlip:GFP (top and bottom), Spd2:RFP (top, left) and MyoII:3xmKate2 (top middle and top right). Spd2:RFP labels centrosomes. Yellow arrowheads: accumulations of RhoGAP68F:GFP around the centrosomes, and accumulations of RhoGAP1A:GFP and Rlip:GFP around the nucleus.

(D) xy images at the level of the spindle of Tum:GFP, RhoGAPp190:GFP, RhoGAP1A:GFP (top and bottom) and Myo:3xmKate2 (top) in mitotic cells in the notum. Yellow arrowheads indicate GFP accumulations at the spindle.

(E) xy images at the level of the spindle of Zir:GFP (top and bottom) and Myo:3xmKate2 (top) in mitotic cells in the FE. Yellow arrowheads indicate Zir:GFP enrichment around the spindle.

(F) xy images of RhoGEF4:GFP, RhoGAP54D:GFP (top and bottom) and MyoII:3xmKate2 (top) during metaphase in the notum.

(G) xy images of Mbc:GFP and CG46491:GFP (top and bottom) and MyoII:3xmKate2 (top) during anaphase in the FE. Yellow arrowheads: Mbc:GFP enrichment or CG46491:GFP depletion at polar regions of the cortex.

(H) yz images of Graf:GFP, Zir:GFP, Mbc:GFP and Ziz:GFP, and xy images of RhoGEF64C:GFP, Zir:GFP (top and bottom) and MyoII:3xmKate2 (top) during cytokinetic ring constriction in the notum. White arrowheads: contractile ring. Yellow arrowheads: Graf:GFP and Zir:GFP accumulations at the cytokinetic ring; Mbc:GFP and Ziz:GFP accumulations below the cytokinetic ring; RhoGEF64C:GFP and Zir:GFP accumulations around the apical contractile ring.

(I) yz images of CdGAPr:GFP, RhoGEF4:GFP (top and bottom) and MyoII:3xmKate2 (top) during cytokinetic ring constriction in the FE.

(J) xy images of OCRL:GFP, Zir:GFP, RhoGEF64C:GFP and yz images of CG43102:GFP (top and bottom), and MyoII:3xmKate2 (top) during late cytokinesis in the notum. White arrowheads: midbody. Yellow arrowheads: CG43102:GFP accumulation basal to the midbody.

(K) xy images of Graf:GFP, CdGAPr:GFP, Exn:GFP (top and bottom) and MyoII:3xmKate2 (top) during cytokinesis in the notum. White arrowheads: cytokinetic ring. Yellow arrowheads: Graf:GFP, CdGAPr:GFP and Exn:GFP accumulations at the rim of the cytokinetic ring.

(L) Apical (left) and basal (right) xy images of Cdep:GFP (top and bottom) and MyoII:3xmKate2 (top) during daughter junction formation in the FE. White arrowheads: midbody. Yellow arrowheads: Cdep:GFP accumulation along the daughter interface from the apical to the basal level.

(M) xy images of CG43102:GFP, Exn:GFP, GEFMeso:GFP (top and bottom) and MyoII:3xmKate2 (top) during late cytokinesis and *de novo* daughter cell junction formation in the notum. White arrowheads: midbody.

(N) xy images of RhoGAP5A:GFP, RhoGAP15B:GFP, Zir:GFP, RhoGAP54D:GFP, CdGAPr:GFP (top and bottom) and MyoII:3xmKate2 (top) during late cytokinesis in the FE. White arrowheads: midbody. Yellow arrowheads: new interface.

Scale bars: 5 μ m

See also Video S1, Data S1A,B and the [website](#).

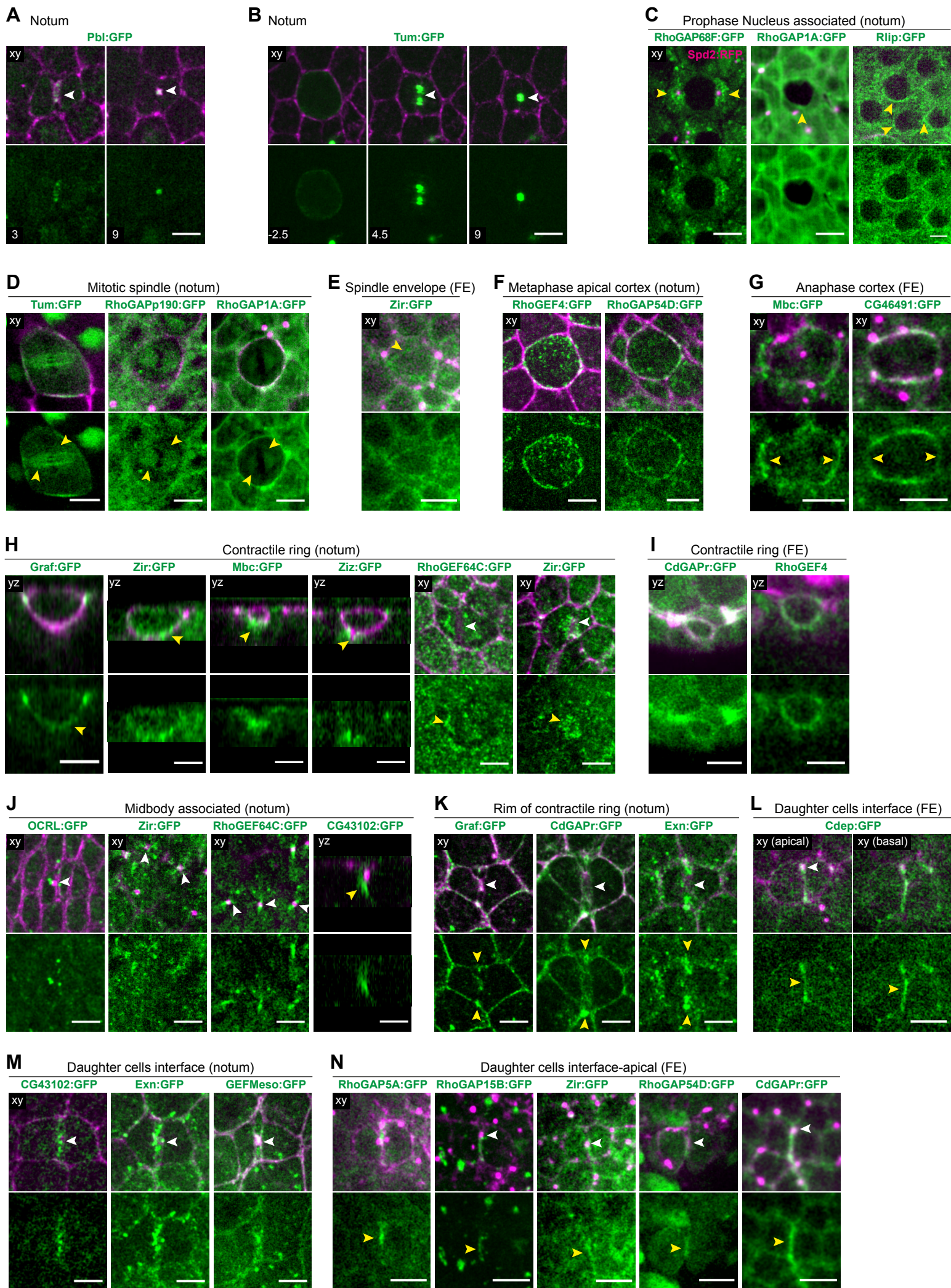


Figure S4: Analysis of Cysts localization and function, related to Figure 2

Unless otherwise indicated, all confocal images are apical top views at the level of the AJ in the notum, and time (min, indicated in the lower left image corner) is set to 0 at the onset of cytokinesis marked by the initial deformation of AJ by the constriction of the cytokinetic ring.

(A) Time-lapse images of Cysts:GFP (top and bottom) and MyoII:3xmKate2 (top) during cytokinesis in the FE. Yellow arrowheads: Cysts:GFP accumulations at the rim of the cytokinetic ring.

(B) Time-lapse images of Cysts:GFP and MyoII:3xmKate2 during cytokinesis in the notum. Laser ablation of the ring was performed in the dashed outlined region. Yellow arrowheads: Cysts:GFP at the rim of the cytokinetic ring in neighbors of a dividing cell before ablation and upon ablation. Yellow open arrowheads: reduced Cysts:GFP accumulation in cells neighboring the ring ablated dividing cell. Orange arrowheads: Cysts:GFP accumulation at the rim of the cytokinetic ring in neighbors of a dividing ctrl cell without ring ablation. 26 out 32 (81%) dividing cells exhibited a decrease accumulation of Cysts: GFP after ring ablation.

(C) Image of Cysts:GFP and MyoII:3xmKate2 in ctrl and *Ecad^{RNAi}* interphasic cells. *Ecad^{RNAi}* cells are marked by the expression of CAAX:tBFP (not shown), and a yellow dashed line outlines the boundary between ctrl and *Ecad^{RNAi}* cells. Inset: close-up on the region outlined by the dashed white box.

(D) Kymographs of Cysts:GFP (top and bottom) and MyoII:3xmKate2 (top and middle) within the region outlined in the inset in (C). Yellow arrowheads indicate the flows of MyoII:3xmKate2 and Cysts:GFP towards the medial apical region of the *Ecad^{RNAi}* cell. Time (min) is set to 0 at the beginning of the kymograph.

Scale bars: 5 μ m (A, B, C), 1 μ m (inset in C).

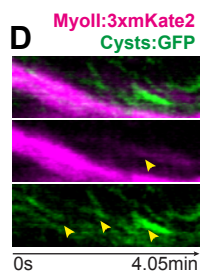
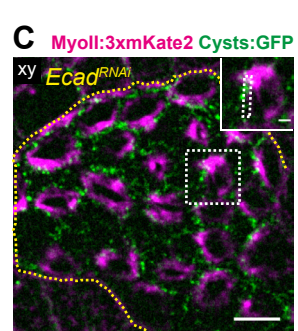
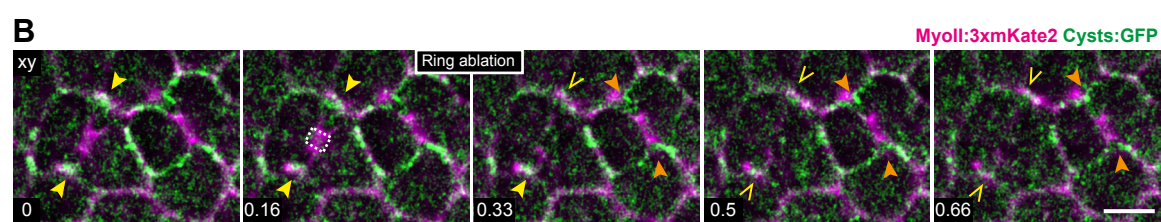
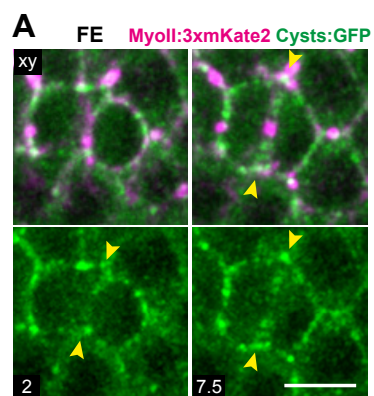


Figure S5: RhoGEF4 localization and function in epithelial tissues, related to Figure 4.

Unless otherwise indicated, all confocal images are apical top views at the level of the AJ in the notum, and time (min, indicated in the lower left image corner) is set to 0 at the onset of cytokinesis marked by the initial deformation of AJ by the constriction of the cytokinetic ring. For details on quantifications, see STAR Methods.

(A) xy images at the level of the nuclei of RhoGEF4:GFP (top and bottom) and Lamin:TagRFP (top) in interphase cells.

(B) yz time-lapse images of RhoGEF4:GFP (top and bottom) and MyoII:3xmKate2 (top) from interphase to early cytokinesis. yz sections are shown at the level of the contractile ring. Time (min) is set to 0 at the start of the time-lapse sequence. Yellow arrowhead: AJ.

(C) Time-lapse images of RhoGEF4:GFP (top and bottom) and MyoII:3xmKate2 (top) during cell division in the FE. White arrowhead: midbody. White dashed box: daughter cell interface.

(D) Time-lapse images of Ecad:GFP and MyoII:3xmKate2 in ctrl and *rhogef4* dividing cells in the FE. Time is set to 0 at the end of ring contraction. White arrowhead: midbody. Inset: daughter cell interface for the Ecad:GFP channel.

(E) Box plot of initial AJ length (median \pm interquartile range) in ctrl and *rhogef4* dividing cells in the FE. Junction length measurements were performed 10 min after the end of ring constriction.

(F) Time-lapse images of MyoII:3xmKate2 (top) and clonally expressed RhoGEF4:GFP (top and bottom) and His2A:RFP (top) from early to late cytokinesis. Yellow dashed line: boundary between the His2A:RFP (top) or RhoGEF4:GFP (bottom) clone cells. Yellow arrowheads: accumulation of RhoGEF4:GFP on both sides of the contractile ring and daughter cell interface in a RhoGEF4:GFP expressing dividing cell at the clone border. Note that in His2A:RFP clonal cells that do not have a RhoGEF:GFP transgene, a GFP dotted signal can be observed.

(G) Time-lapse images of MyoII:3xmKate2 (top) and clonally expressed RhoGEF4:GFP (top and bottom) and His2A:RFP (top) from early to late cytokinesis. Yellow dashed line: boundary between the His2A:RFP (top) or RhoGEF4:GFP (bottom) clone cells. Yellow open arrowhead: absence of RhoGEF4:GFP accumulation at the ring, midbody and daughter cell interface in a His2A:RFP expressing dividing cell, neighboring a RhoGEF4:GFP clonal cell. White asterisks: mitotic chromosomes labelled by His2A:RFP. Note that in His2A:RFP clonal cells that do not have a RhoGEF4:GFP transgene, a GFP dotted signal can be observed.

(H) Time-lapse images of Ecad:GFP, MyoII:3xmKate2 and nls:GFP in a *rhogef4* dividing cell surrounded by two ctrl neighboring cells. *rhogef4* cells are marked by the absence of nls:GFP expression, and a yellow dashed line marks the boundary between ctrl and *rhogef4* cells. Note that nls:GFP is not visible since the nuclei are located more basally. White arrowheads: midbody. Yellow arrowheads: MyoII accumulation in the neighboring cells and prospective position of *de novo* daughter-daughter cell junction.

(I) Box plot of daughter-daughter interface angle (median \pm interquartile range) at 80% of apical ring contraction and at midbody formation in ctrl and *rhogef4* dividing cells in the notum.

(J) Box plot of ring contraction rate (median \pm interquartile range) in ctrl and *rhogef4* dividing cells in the notum.

(K) Graph of the nls:GFP cytoplasmic/nuclear ratio (mean \pm SEM) during late cytokinesis in ctrl and *rhogef4* cells in the notum.

(L) Graph of Lamin:TagRFP levels (mean \pm SEM) at the daughter cells nuclear envelope during cytokinesis in ctrl and *rhogef4* cells in the notum.

Scale bar: 5 μ m (A, B, C, D, F, G, H). Mann-Whitney test: NS: non significant, **: $p < 0.01$.

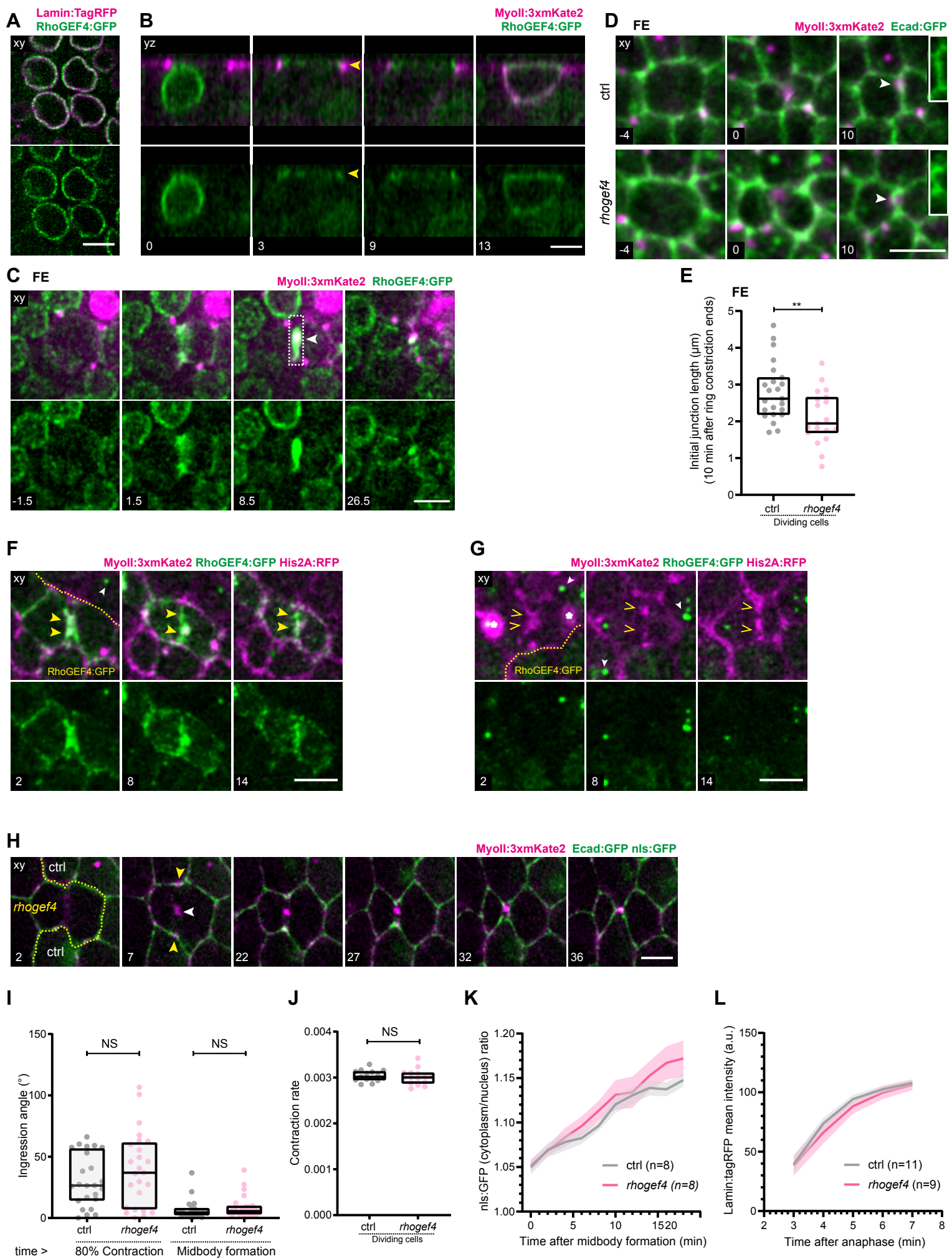


Figure S6: Analyses of RhoGEF4 function in epithelia, related to Figures 4, 5 and 6

All images are apical top views at the level of the AJ. In (H, I), the dividing and daughter cells are coloured in pink and neighboring cells in yellow. Unless otherwise indicated, time (min, indicated in the lower left image corner) is set to 0 at the onset of cytokinesis marked by the initial deformation of AJ by the constriction of the cytokinetic ring.

(A) Graph of the initial AJ length as a function of the time of AJ formation in ctrl and *rhogef4* dividing cells in the notum. R^2 values for linear regressions are indicated.

(B) Graph of Ecad:GFP levels at the daughter cell interface (mean \pm SEM) during *de novo* junction formation in ctrl and *rhogef4* cells in the FE. Time is set to 0 at the end of ring constriction.

(C) Time-lapse images of clonally expressed PH:GFP and PH:chFP in a ctrl dividing cell (marked by PH:GFP) surrounded by *rhogef4* cells (marked by PH:chFP) in the notum. Time (min) is set to 0 at the time of full neighboring membrane ingression. The dividing cell membranes are only shown in the first panel. *rhogef4* cells are marked by the absence of PH:GFP expression, and the yellow dashed line outlines the boundary between *rhogef4* and ctrl cells. Yellow arrowheads: position of the tip of the neighboring membranes inserted between the two daughter cells.

(D) Box plot of the duration of ctrl or *rhogef4* neighboring cell membrane withdrawal (median \pm interquartile range) from ctrl daughter cell apical interfaces in the notum. The ctrl data is the same shown in Fig4E.

(E) Time-lapse images of MyoII:3xmKate2 and Ani-RBD:GFP for ctrl and *rhogef4* dividing cells during cytokinesis in the notum. Inset: close-up on the Ani-RBD:GFP signal at the apical contractile ring and midbody.

(F) Box plot of Ani-RBD:GFP intensity (median \pm interquartile range) at the apical contractile ring of ctrl or *rhogef4* cells in the notum.

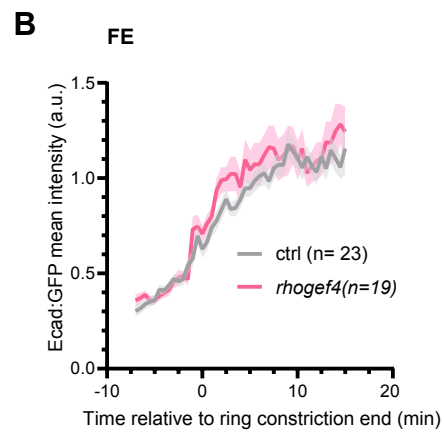
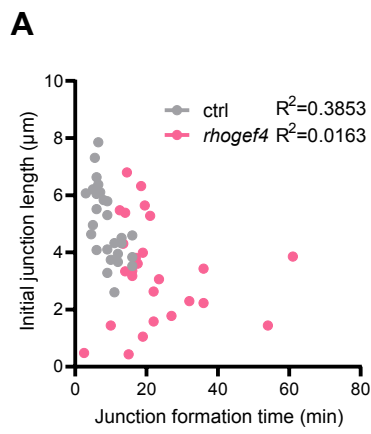
(G) Graph of the timing of the initial AJ formation in *rhogef4* dividing cells for which a d-d or a n-n junction are initially formed, in the notum epithelium. The time (min) is set to 0 at midbody formation.

(H) Time-lapse images of Ecad:GFP from cytokinesis onwards in wt or *rhogef4* animals in the pupal wing epithelium.

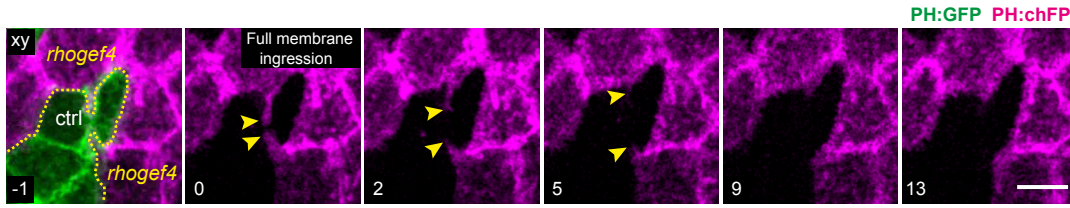
(I) Time-lapse images of Ecad:GFP from cytokinesis onwards in wt or *rhogef4* animals in the pupal histoblast nest epithelium.

(J) Graph of the frequency of total n-n junctions formed upon cell division in wt and *rhogef4* mutant animals in the pupal wing and histoblast epithelial tissues.

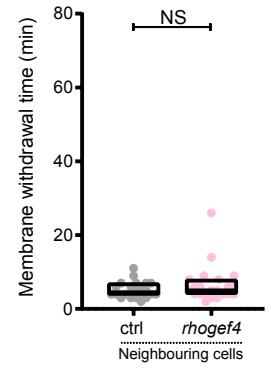
Scale bar: 5 μ m (C, E, H, I), 1 μ m (inset in E). Mann-Whitney test, NS: non significant (D, F, G). Z-score proportion test (J). *: $p < 0.05$.



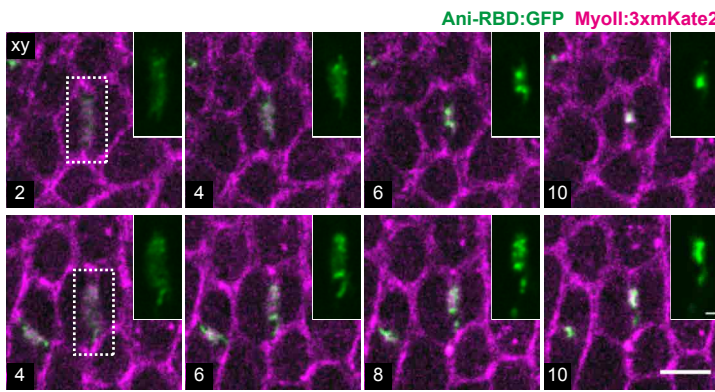
C



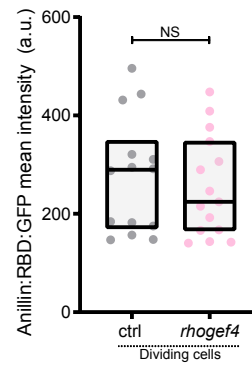
D



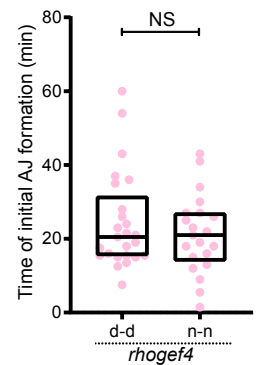
E



F

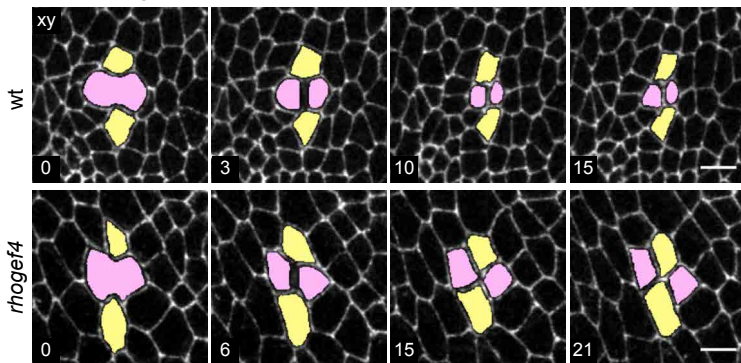


G



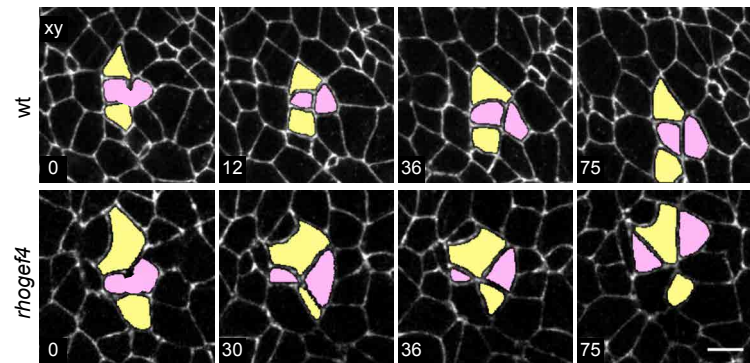
H Pupal wing

Ecad:GFP



I Pupal histoblast

Ecad:GFP



J

